

Solar Magnetic Field Profiles and SuperKamiokande Data

João Pulido

Centro de Física das Interações Fundamentais
Instituto Superior Técnico
Av. Rovisco Pais, 1096 Lisboa Codex, Portugal

September 11, 2018

Abstract

The distortion of the energy spectrum of recoil electrons in SuperKamiokande resulting from several solar magnetic field profiles that are consistent with data and standard solar models is investigated. The aim is to provide a test of the general common features of these field profiles derived in a previous work on the basis of the resonant spin flip flavour mechanism. It is found that the distortion may be visible in the data, becoming possibly clearer when the energy threshold succeeds in being reduced and distinct from the ones resulting from oscillations.

The possibility that neutrinos have a magnetic moment [1] may provide a unique insight on the inner solar magnetic field, with the resonant spin flip flavour conversion of neutrinos [2] taken as the main origin of the solar neutrino deficit. In general terms this deficit consists in the fact that too few neutrinos are being detected [3] - [6] as compared to the theoretical predictions [7] - [14]. The location of the resonance inside the Sun in a resonant process is uniquely fixed for a given flavour mass square difference by the neutrino energy, so that a high suppression at a given energy range is interpreted in the resonant spin flip flavour as a high field intensity over a corresponding spatial range. In this way it was shown [15] that the results from the four solar neutrino experiments [3] - [6] are indicative of an average field intensity rising sharply by at least a factor 6 - 7 over a distance no longer than 7 - 10% of the solar radius, decreasing then gradually towards the surface. Helioseismology suggests that such a sharp rise must lie around the upper layers of the radiative zone and the bottom of the convective zone [16], with the field reaching the order of 10^5G at its maximum. The required order of magnitude of the electron neutrino magnetic moment is from a few times $10^{-13}\mu_B$ to its laboratory upper bounds [17].

This magnetic field scenario is consistent with but obviously in no way implied by the data on solar neutrinos. Its verification can only be provided by the second generation high precision experiments like SuperKamiokande [18] and SNO [19].

In this paper we investigate the distortion of the recoil electron energy spectrum in the SuperKamiokande experiment associated with the general magnetic field profile described above. The high statistics of SuperKamiokande, together with the lowering of their recoil electron energy spectrum will hopefully make it possible, if this scenario is realistic, to trace and identify its characteristic distortion.

The starting point is the true event rate in SuperKamiokande which we will denote by $S'(T')$ and is given by [20]

$$S'(T') = \int_{E_{\nu m}}^{E_{\nu M}} dE_{\nu} \left(P(E_{\nu}) \frac{d^2\sigma_W}{dT' dE_{\nu}} + \frac{d^2\sigma_{-EM}}{dT' dE_{\nu}} \right) f(E_{\nu}) \quad (1)$$

Here T' is the true recoil electron kinetic energy, $f(E_{\nu})$ is the energy distribution ¹ of ^8B neutrinos [22] and $P(E_{\nu})$ is the survival probability for neutrinos with energy E_{ν} . The lower and upper integration limits in eq.(1) are determined respectively by the kinematical inequality

$$E_{\nu} \geq \frac{T' + \sqrt{T'^2 + 2m_e T'}}{2} \quad (2)$$

and the maximum ^8B neutrino energy [22]

$$E_{\nu M} = 15\text{MeV}. \quad (3)$$

The weak and electromagnetic spin flip parts of the $\nu_e e^- \rightarrow \nu_e e^-$ cross section are given by the expressions [20]

$$\frac{d^2\sigma_W}{dT' dE_{\nu}} = \frac{G_F m_e}{2\pi} \left((g_V + g_A)^2 + (g_V - g_A)^2 \left(1 - \frac{T'}{E_{\nu}}\right)^2 - (g_V^2 - g_A^2) \frac{m_e T'}{E_{\nu}^2} \right) \quad (4)$$

¹The uncertainties in the solar magnetic field do not justify replacing the more recent standard neutrino energy spectrum from ^8B decay [21] for the one used throughout this paper [22].

$$\frac{d^2\sigma_{-EM}}{dT'dE_\nu} = f_\nu^2 \frac{\pi\alpha^2}{m_e^2} \left(\frac{1}{T'} - \frac{1}{E_\nu} \right) \quad (5)$$

in standard notation and with f_ν being the neutrino magnetic moment in Bohr magnetons. We assume vanishing mean square radius for the neutrino, so that the contributions of the spin non-flip and interference cross sections are absent, and take for $\nu = \nu_e$

$$g_V = \frac{1}{2} + 2\sin^2\theta_W \quad , \quad g_A = \frac{1}{2} \quad (6)$$

with $\sin^2\theta_W = 0.23$.

The true (physical) event rate $S'(T')$ given by (1) is in fact smeared by the energy resolution function of the detector $R(T', T)$ [18] and the measured event rate is instead

$$S(T) = \int_0^{T'_M} S'(T') R(T', T) dT' \quad (7)$$

where T is the measured recoil kinetic energy,

$$T'_M = \frac{2E_{\nu_M}^2}{2E_{\nu_M} + m_e} \quad (8)$$

(from inequality (2)) and [18]

$$R(T', T) = \frac{1}{\Delta_{T'}\sqrt{2\pi}} \exp\left(-\frac{(T' - T)^2}{2\Delta_{T'}^2}\right). \quad (9)$$

In equation (9) the parameter $\Delta_{T'}$ denotes the energy dependent 1σ width of the resolution function,

$$\Delta_{T'} = \Delta_{10} \sqrt{\frac{T'}{10MeV}}. \quad (10)$$

Currently for SuperKamiokande $\Delta_{10} = 1.5MeV$.

For the survival probability in equation (1), $P(E_\nu)$, we will use the Landau Zener approximation whereby [23]

$$P(E_\nu) = P_{LZ}(E_\nu) = \exp\left(-\pi \frac{2\mu_\nu^2 B^2}{\frac{\Delta^2}{2E_\nu}} 0.09R_S\right) \quad (11)$$

with B_{res} denoting the magnetic field at the resonance (critical) point,

$$x_{res} = \frac{r}{R_S} = 0.09 \log \frac{\frac{5}{3\sqrt{2}} 2.11 \times 10^{-11} eV}{\frac{\Delta^2}{2E_\nu}}, \quad (12)$$

Δ^2 the neutrino flavour mass square difference, μ_ν the neutrino magnetic moment and R_S the solar radius. In the present investigation we assume a vanishing vacuum mixing angle, so we will be solely analysing the joint effect of the neutrino magnetic moment and solar magnetic field.

The values of the event rate $S(T)$ given by expression (7) with $S'(T')$ and $R(T', T)$ defined by (1) and (9) respectively will now be confronted with the corresponding event

rate $S_{st}(T)$ for standard neutrinos ($\mu_\nu = f_\nu = 0$) for which the survival probability is obviously unity. We have

$$S_{st}(T) = \int_0^{T_M} S'_{st}(T') R(T', T) dT' \quad (13)$$

with

$$S'_{st}(T') = \int_{E_{\nu m}}^{E_{\nu M}} dE_\nu \frac{d^2\sigma_W}{dT' dE_\nu} f(E_\nu). \quad (14)$$

The ratio between equations (7) and (13) provides a measure of the deviation of the recoil energy spectrum relative to the corresponding spectrum for standard neutrinos. For high enough experimental sensitivity and sufficiently low energy threshold, as will be seen, this deviation will become apparent, thus constituting a signature of the suppression process occurring in the Sun. Another way of expressing this signature is through the distortion of the electron energy spectrum. To this end, choosing to normalize the above ratio between (7) and (13) to its value at $T = 8$ MeV, we will express the distortion as

$$D(T) = \frac{S(T)}{S_{st}(T)} \times \frac{S_{st}(8)}{S(8)}. \quad (15)$$

We consider the general field profile described in the introduction with all its possible variants, together with the corresponding solution ranges in terms of μ_ν and Δ^2 , compatible with solar neutrino data [3] - [6] and standard solar models [7], [10] - [14] (see table I). All these fields satisfy the general feature of having a sharp rise by nearly an order of magnitude or more across the upper radiation zone and the bottom of the convection zone, decreasing smoothly towards the surface with an upward facing concavity or a linear decrease. (A downward facing concavity must be excluded [15]). The first five were taken directly from ref. [15] and the last one was added in order to account for the possibility of a $3 \times 10^5 G$ field at the bottom of the convective zone [16].

It should be emphasized that the lowering of the energy threshold in the experiment is essential in order to "magnify" the distortion effect for a given solar field distribution. In fact, for all field distributions, the survival probability decreases rapidly with decreasing E_ν (see fig. 1 for a typical example). By lowering the recoil electron energy threshold $E_{e min}$ ($T_{min} = E_{e min} - m_e$), the lower integration limit in equation (1) decreases, so the smaller probabilities become more predominant in the integration, providing a stronger reduction effect in $S(T)$ with respect to $S_{st}(T)$ at lower T .

The distortion of the recoil electron energy spectrum (eq. (15)) for the six field profiles considered in table I is shown in figs. (2) through (7). The range of solutions in terms of μ_ν and Δ^2 is limited by the values denoted (a), (b) in each case, the solid lines corresponding to cases (a) and the dashed lines to cases (b). Hence the range of possible distortions for each field profile is limited by the two curves. The "magnification" effect in the distortion for a lowering T is apparent from these figures.

As far as time variations of neutrino flux with solar activity are concerned, no other suppression mechanism apart from the magnetic moment one can reflect them, since solar activity is correlated with magnetic field intensity. It has not become clear as yet whether Homestake [3], the only experiment claiming such time variations in its data so far, shows any evidence of them. These data are consistent with no anticorrelation with the 11 year solar cycle [24], [25], but other periodic time dependence of the data may exist [25].

Only the second generation of experiments, namely SuperKamiokande [18] may provide a clarification. The highest energy 8B neutrinos ($E_\nu \geq 8MeV$), which are hardly suppressed (see fig. 1) and therefore whose resonances are strongly non-adiabatic, cannot show any sign of anticorrelation with solar activity and magnetic field. Once again it is only in the low E_ν sector and therefore in the lowest electron energy T sector of the data that this effect may appear. A change in the average magnetic field by a factor of approximately 3, as in the cases (5) and (6) of table I (see figs. 6 and 7 respectively), clearly shows up in the distortion, with the average larger field (6) of the same shape as (5) corresponding to a larger distortion. So the spectrum distortion of the recoil electron kinetic energy is correlated with the solar activity: the more intense the solar activity, the larger the distortion. Its signature is also characteristically different from the one originated by the vacuum oscillation, the large and the small mixing angle solutions [26], [27].

To conclude, all possible solar magnetic field profiles that are compatible with the data from the first generation of solar neutrino experiments provide a distortion of the kinetic energy spectrum of recoil electrons that appears to be detectable and distinguishable in SuperKamiokande and increases with solar activity. To this end, it will be of primordial importance to decrease as much as possible the energy threshold of the experiment.

References

- [1] M. B. Voloshin, M. I. Vysotsky and L. B. Okun, Sov. J. Nucl. Phys. **44** 440 (1986); M. B. Voloshin and M. I. Vysotsky *ibid.*, **44** 544 (1986).
- [2] C. S. Lim and W. J. Marciano, Phys. Rev. **D 37** 1368 (1988); E. Kh. Akhmedov, Phys. Lett. **B 213** 64 (1988); E. Kh. Akhmedov, Sov. J. Nucl. Phys. **48** 382 (1988).
- [3] Homestake Collaboration: R. Davis Jr., Prog. Part. Nucl. Phys. **32** 13 (1994); K. Lande and P. S. Wildenhain in Neutrino '96 , Proceedings of the 17th International Conference on Neutrino Physics and Astrophysics, Helsinki, Finland, ed. by K. Enqvist, K. Huitu and J. Maalampi (World Scientific, Singapore, 1997) p. 25.
- [4] Kamiokande Collaboration: Y. Suzuki, Nucl. Phys. **38** 54 (1995).
- [5] Gallex Collaboration: P. Anselmann et al., Phys. Lett. **B 342** 440 (1995).
- [6] SAGE Collaboration: J. N. Abdurashitov et al., Phys. Lett. **B328** 234 (1994).
- [7] J. N. Bahcall and M. H. Pinsonneault, Rev. Mod. Phys. **67** 781 (1995).
- [8] J. N. Bahcall, S Basu and M. H. Pinsonneault, Phys. Lett. **B433** 1 (1998).
- [9] A. S. Brun, S. Turck-Chieze and P. Morel, astro-ph/9806272.
- [10] S. Turck-Chieze, I. Lopes, Ap. J. **408** 347 (1993).
- [11] S. Turck-Chieze et al., Ap. J. **335** 415 (1988).

- [12] C. R. Profitt, Ap. J. **425** 849 (1994).
- [13] O. Richard et al., Astron. Astrophys. **312** 1000 (1996).
- [14] S. Degl’Innocenti et al., Astron. Astrophys. Suppl. Ser. **123** 1 (1997).
- [15] J. Pulido, Phys. Rev. **D57** 7108 (1998).
- [16] E. N. Parker in "The Structure of the Sun", Proceedings of the VI Canary Islands School, Ed. T. Roca Cortés and F. Sanchez, Cambridge University Press 1996 p. 299.
- [17] Particle Data Group, R. M. Barnett et al., Phys. Rev **D 54** 1 (1996).
- [18] Y. Totsuka, to appear in the Proceedings of the 18th Texas Symposium on Relativistic Astrophysics, December 15-20, 1996, Chicago, Illinois, eds. A. Olinto, J. Frieman and D. Shramm (World Scientific, Singapore).
- [19] A. B. McDonald, in Particle Physics and Cosmology, Proceedings of the 9th Lake Louise Winter Institute, eds. A. Astbury et al. (World Scientific, Singapore) p.1.
- [20] J. Pulido and Ana M. Mourão, Phys. Rev. **D 57** 1794 (1997) and references therein.
- [21] J. N. Bahcall et al., Phys. Rev. **C 54** 411 (1996).
- [22] J. N. Bahcall and R. K. Ulrich, Rev. Mod. Phys. **60** 297 (1988).
- [23] J. Pulido, Phys. Rep. **211** 167 (1992).
- [24] G. Walther, Phys. Rev. Lett. **79** 4522 (1998).
- [25] H. J. Haubold, lectures at Workshop on Data Analysis Techniques, Brazil, November 1997, astro-ph/9803136.
- [26] J. N. Bahcall, lectures at the XXV SLAC Summer Institute on Particle Physics "Physics of Leptons", Aug. 4-15 1997, to be published in a SLAC Report, hep-ph/9711358.
- [27] P. I. Krastev. A. Yu. Smirnov, Phys. Lett. **B 338** 282 (1994).

B (Gauss)	x	solution	
		(a)	(b)
0	$0 \leq x \leq 0.7$	$3.1 \times 10^{-12} \mu_B \leq \mu_\nu \leq 3.8 \times 10^{-12} \mu_B$	
$2 \times 10^6(x - 0.7)$	$0.7 \leq x \leq 0.75$	$6.33 \times 10^{-9} eV^2 \leq \Delta^2 \leq 6.56 \times 10^{-9} eV^2$	
10^5	$0.75 \leq x \leq 0.8$		
$10^5 - 4.9 \times 10^5(x - 0.8)$	$0.8 \leq x \leq 1$		
9.4×10^4	$x \leq 0.645$	$\mu_\nu = 10^{-12} \mu_B$	
$9.32 \times 10^6(x - 0.645) + 9.4 \times 10^4$	$0.645 \leq x \leq 0.71$	$1.5 \times 10^{-8} eV^2 \leq \Delta^2 \leq 1.91 \times 10^{-8} eV^2$	
$-3.4 \times 10^6(x - 0.71) + 7 \times 10^5$	$0.71 \leq x \leq 0.91$		
$-2 \times 10^5(x - 0.91) + 2 \times 10^4$	$0.91 \leq x \leq 1$		
0	$x < 0.71$	$3.4 \times 10^{-11} \mu_B \leq \mu_\nu \leq 1.3 \times 10^{-10} \mu_B$	
$\frac{3.048 \times 10^4}{\cosh[20(x-0.71)]}$	$0.71 \leq x \leq 1$	$1.6 \times 10^{-8} eV^2 \geq \Delta^2 \geq 7.3 \times 10^{-9} eV^2$	
2.16×10^3	$x \leq 0.7105$	$4.1 \times 10^{-12} \mu_B \leq \mu_\nu \leq 6.15 \times 10^{-12} \mu_B$	
$8.7 \times 10^4 \left[1 - \left(\frac{x-0.75}{0.04} \right)^2 \right]$	$0.7105 \leq x \leq 0.7483$	$6.5 \times 10^{-9} eV^2 \leq \Delta^2 \leq 6.9 \times 10^{-9} eV^2$	
$10^5 [1 - 3.4412(x - 0.71)]$	$0.7483 \leq x \leq 1$		
2.16×10^3	$x \leq 0.7105$	$7.2 \times 10^{-12} \mu_B \leq \mu_\nu \leq 2.1 \times 10^{-11} \mu_B$	
$8.7 \times 10^4 \left[1 - \left(\frac{x-0.75}{0.04} \right)^2 \right]$	$0.7105 \leq x \leq 0.7483$	$1.3 \times 10^{-8} eV^2 \geq \Delta^2 \geq 7.3 \times 10^{-9} eV^2$	
$\frac{8.684 \times 10^4}{\cosh[20(x-0.7483)]}$	$0.7483 \leq x \leq 1$		
1.5×10^3	$x \leq 0.7101$	$2.1 \times 10^{-12} \mu_B \leq \mu_\nu \leq 7.3 \times 10^{-12} \mu_B$	
$3 \times 10^5 \left[1 - \left(\frac{x-0.75}{0.04} \right)^2 \right]$	$0.7101 \leq x \leq 0.7483$	$1.3 \times 10^{-8} eV^2 \geq \Delta^2 \geq 7.2 \times 10^{-9} eV^2$	
$\frac{2.9946 \times 10^5}{\cosh[20(x-0.7483)]}$	$0.7483 \leq x \leq 1$		

Table I. Solar magnetic field profiles and corresponding solutions in terms of μ_ν and Δ^2 ranges consistent with data [3] - [6] and standard solar models [7], [10] - [14]. The first five field profiles were proposed in ref. [15] and the last one in the present work using the same data and procedure. Notice that the fourth and fifth only differ in the way they decrease along the convective zone while the last is the previous one beyond the bottom of the convective zone multiplied by a scale factor 3.4.

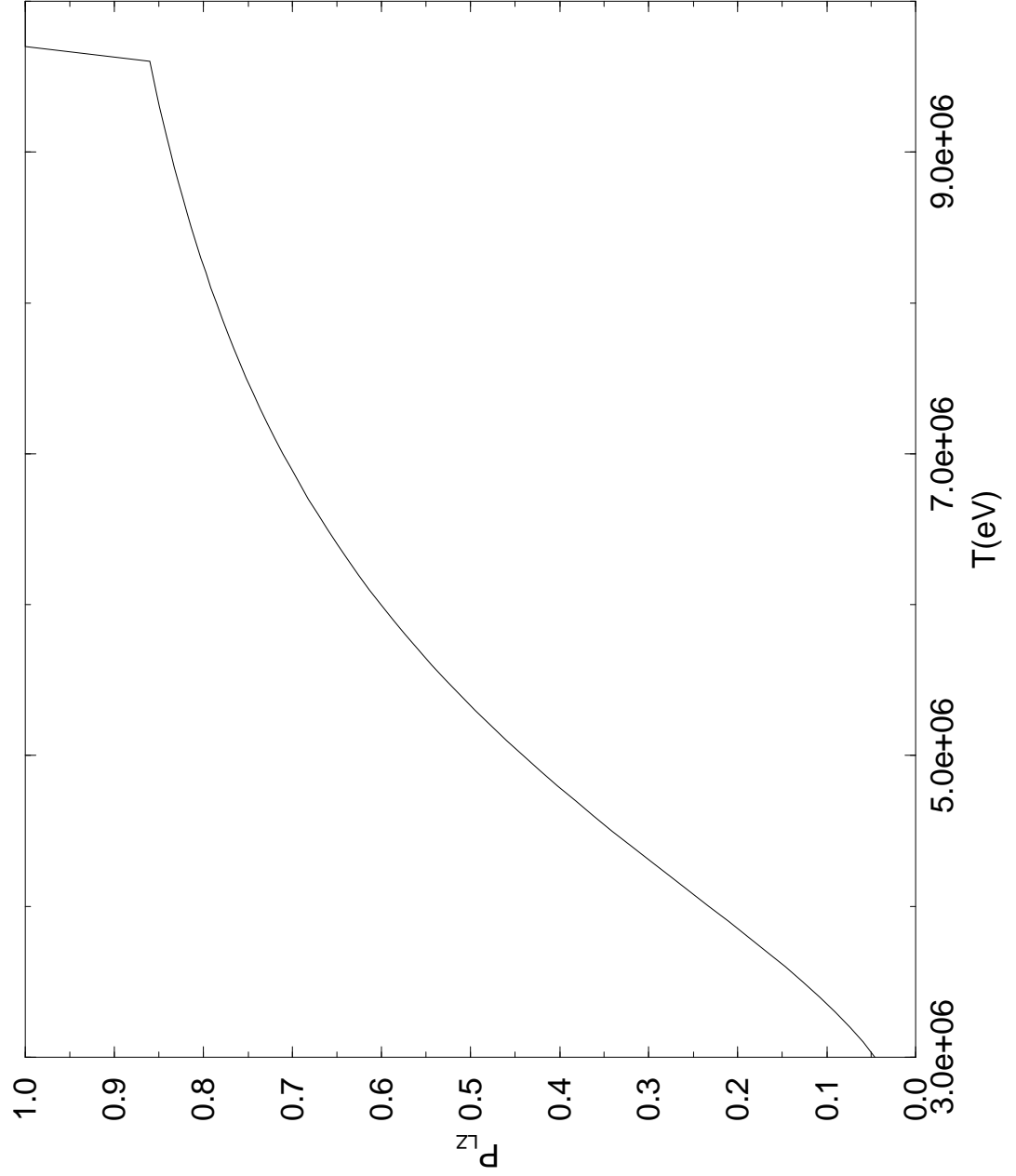


Figure 1: The Landau-Zener probability as a function of neutrino energy E_ν for the last of the field profiles in table I at the upper end solution (case (b)): $\mu_\nu = 7.3 \times 10^{-12} \mu_B$, $\Delta^2 = 7.2 \times 10^{-9} eV^2$. The discontinuity in the derivative at the upper right is related to the sudden drop to zero of the field at the Sun's surface. Units are in eV.

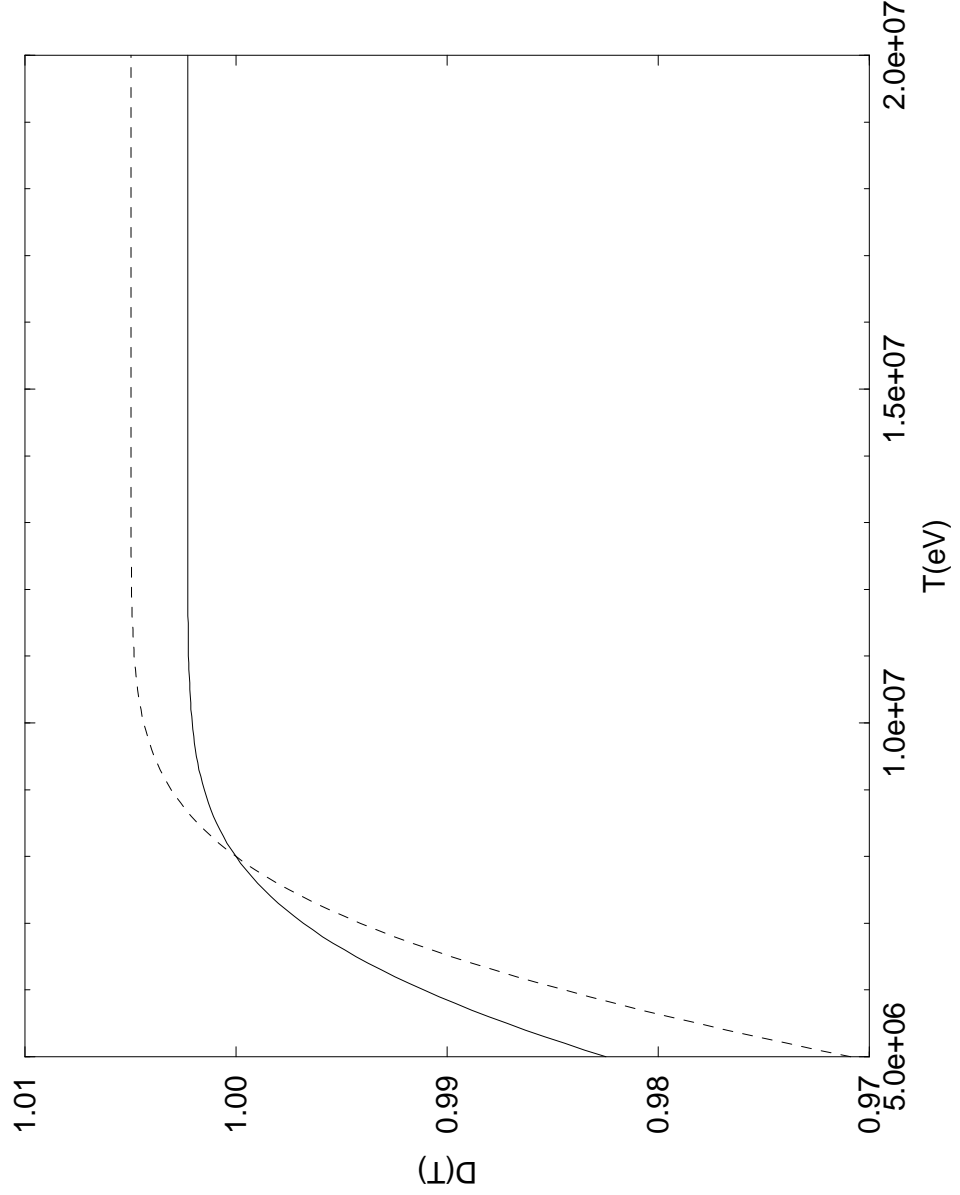


Figure 2: The distortion of the recoil electron kinetic energy spectrum $D(T)$ (eq. (15)) corresponding to the first of the field profiles in table I normalized to its value at $T = 8 \times 10^6 \text{ eV}$. The two ends of the solution range denoted (a) and (b) in table I correspond to the solid and dashed lines respectively. Units are in eV.

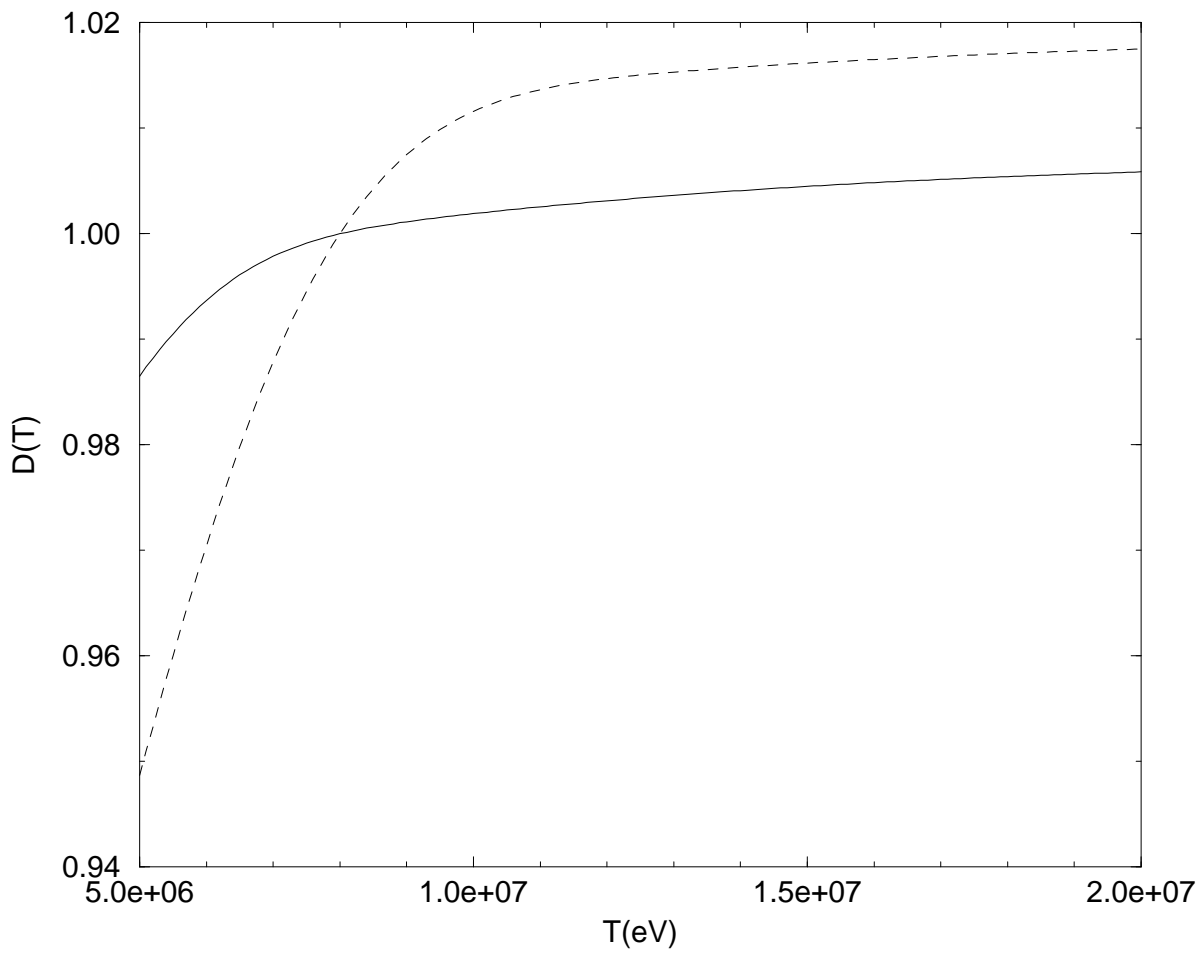


Figure 3: Same as fig. 2 for the second field profile in table I.

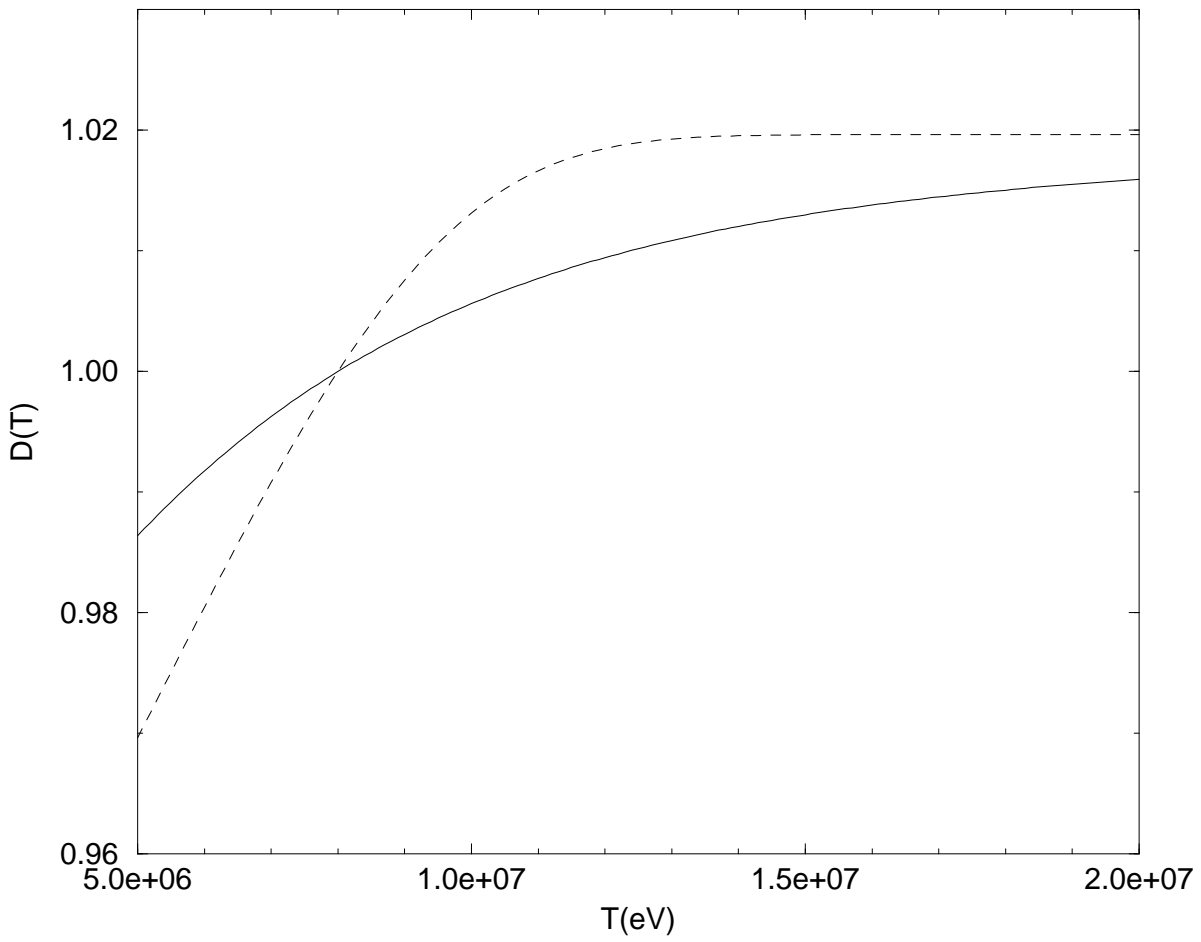


Figure 4: Same as fig. 3 for the third field profile in table I.

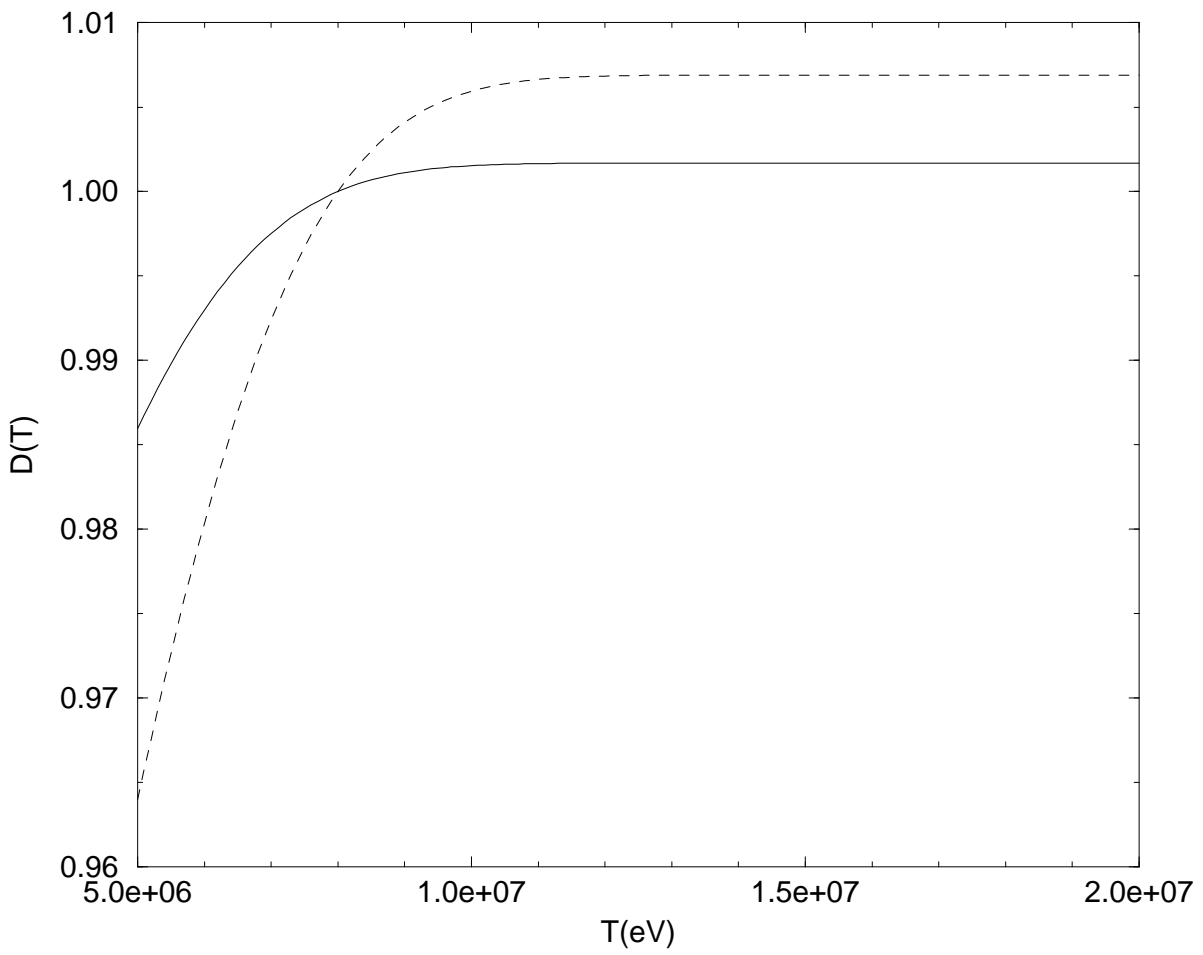


Figure 5: Same as fig. 4 for the fourth field profile in table I.

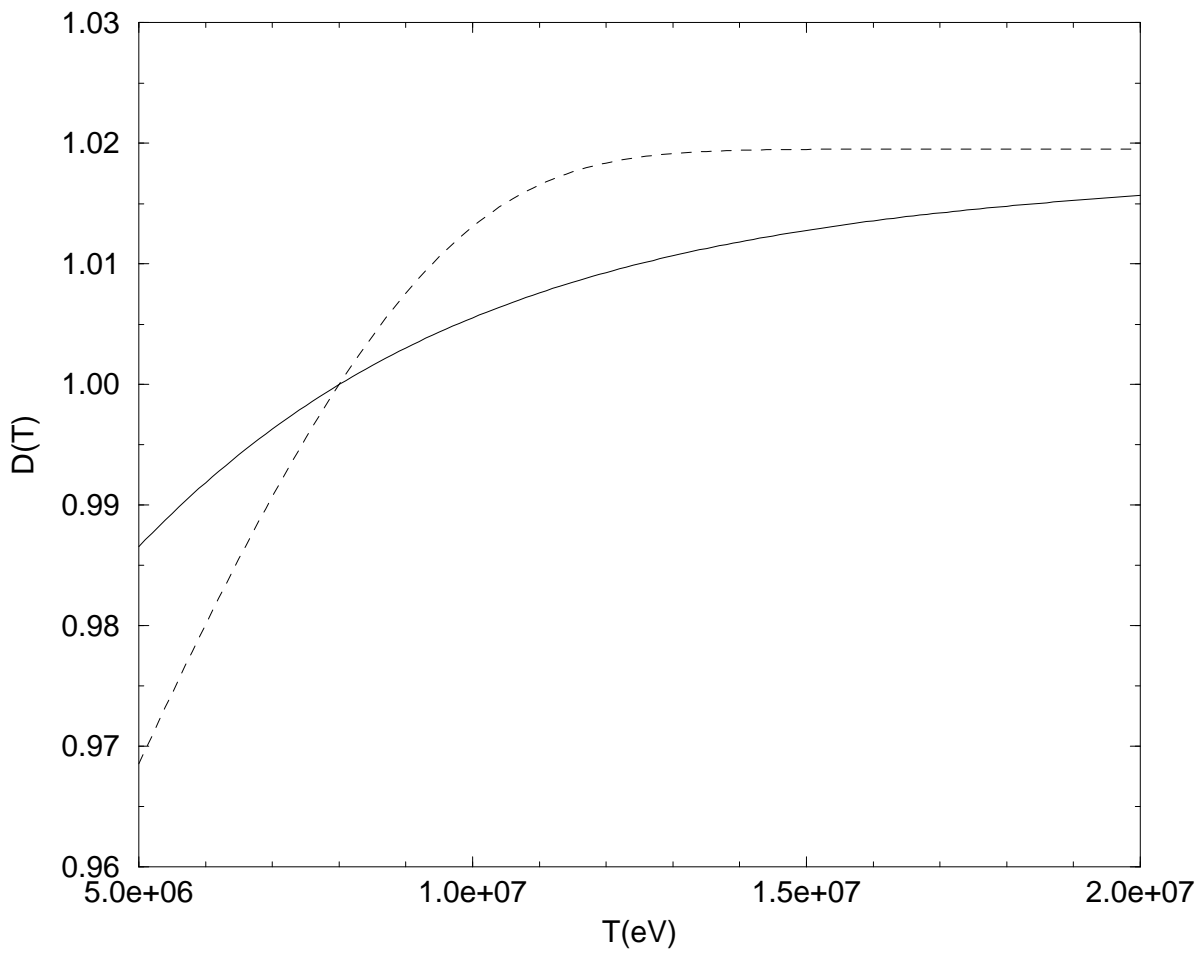


Figure 6: Same as fig. 5 for the fifth field profile in table I.

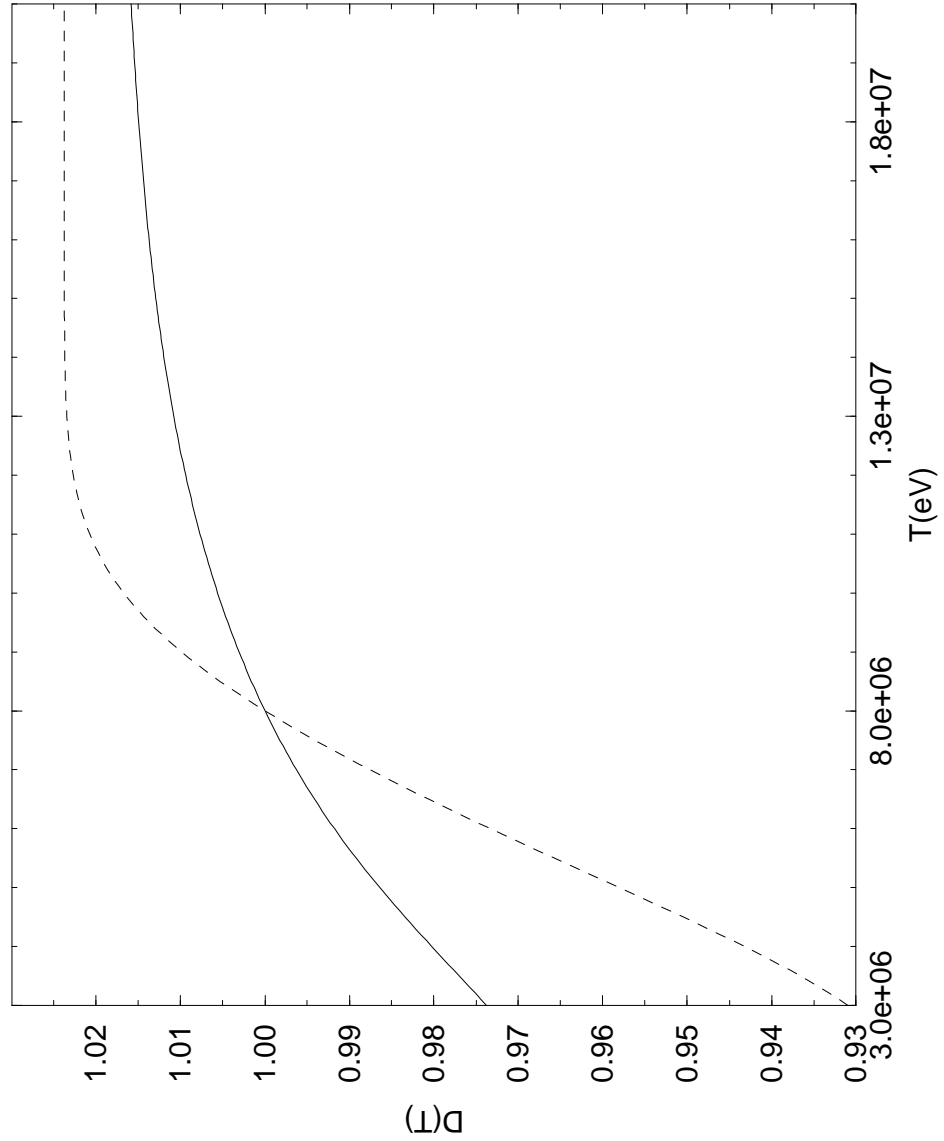


Figure 7: Same as fig. 6 for the sixth field profile in table I. This is essentially the same as the previous one except that it is multiplied by a scale factor of order 3 above the upper radiative zone. Notice that the distortion is slightly increased with respect to fig. 6 indicating a correlation between magnetic field intensity (i. e. solar activity) and distortion.